Laboratori Nazionali di Frascati

Submitted to Physics Letters

LNF-93/035 (P)
5 Luglio 1993

FNT/T-93/20

M. Greco, G. Montagna, O. Nicrosini, F. Piccinini:

RADIATIVE BHABHA SCATTERING AT DAΦNE

PACS.: 12.20-m

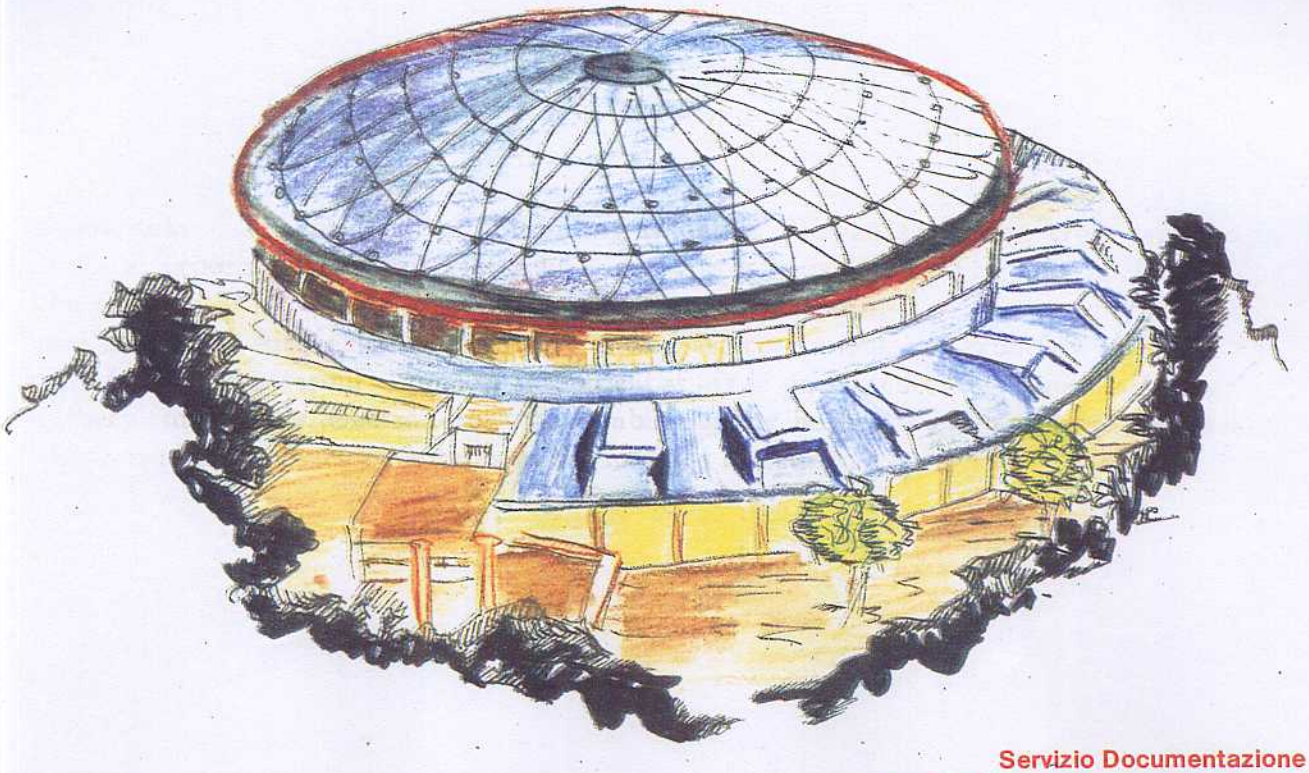

Servizio Documentazione
dei Laboratori Nazionali di Frascati
P.O. Box, 13 - 00044 Frascati (Italy)

INFN - Laboratori Nazionali di Frascati
Servizio Documentazione

LNF-93/035 (P)
5 Luglio 1993

FNT/T-93/20

RADIATIVE BHABHA SCATTERING AT DAΦNE

Mario Greco[a,b], Guido Montagna[a,c], Oreste Nicrosini[a,c] and Fulvio Piccinini[a,c]

a: Università di Pavia, Dipartimento di Fisica Nucleare e Teorica, via A. Bassi n. 6, 27100, Pavia, Italy

b: INFN - Laboratori Nazionali di Frascati, Frascati, Italy

c: INFN - Sezione di Pavia, via A. Bassi n. 6, 27100, Pavia, Italy

Abstract: The problem of computing radiative Bhabha scattering cross sections in realistic experimental setup at DAΦNE energies is considered. The matrix element for the reaction $e^+e^- \to e^+e^-\gamma$ at very small electron scattering angles is computed exactly and compared with existing results. Finite mass corrections are explicitly given for the very forward scattering region. A numerical study is presented for electron single tagging at very small angle, electron-positron double tagging both at small and large angles and electron-photon coincidence rates in the forward direction.

The possibility to observe low energy gamma-gamma processes at DAΦNE provides an important testing ground for Chiral Perturbation Theory [1]. The design machine luminosity $L = 5 \times 10^{32}$ cm^{-2}s^{-1} [2] fully provides the high counting rates which are necessary for the accurate detection of the $\gamma\gamma \to X$ processes ($X = \pi^0, \pi^0\pi^0, ...$) [3]. On the other hand, a careful understanding of the background reactions to tagged e^+e^- events is mandatory for precise experiments and the radiative Bhabha scattering $e^+e^- \to e^+e^-\gamma$ gives the highest number of energetic electrons almost collinear to the incoming beams [4].

A detailed study of this reaction has been performed in the past [5-7]. Differential cross sections in the energy and angle of the emitted particles are available in the literature with the photon spectrum obviously peaked in the forward region. A detailed description of the recoil electron spectrum in coincidence with the photon or positron, as required by small angle tagging facilities, demands however an exact evaluation of the matrix element in the very forward direction, where the momentum transfer is of order m^6/E^4 and the e, γ scattering angles $\vartheta(e,\gamma) \leq 1/\gamma$, with $\gamma = E/m \simeq 10^3$ at DAΦNE.

In these extreme kinematical conditions the expression of the squared matrix element of ref. [7], with the finite mass corrections obviously included, is not accurate enough. Indeed for collinear hard photon emission with the electron in the very forward region, e.g. $\vartheta(e,\gamma) \leq 1/\gamma$, eq. (4.19) of ref. [7] leads to a non physical negative result.

The aim of the present paper is to provide a very accurate description of single photon emission in electron-positron collisions, with particular emphasis in the very forward region. Starting with the exact expression of the matrix element for $m \neq 0$, we study in detail the various differential and total cross sections taking also into account possible kinematical cuts of phenomenological interest for tagging facilities at DAΦNE.

We recover the results of ref. [7] for the squared matrix element when $\vartheta(e) \gg (1/\gamma)$, the single photon spectrum and the total cross section of refs. [5,6] for the unconstrained kinematics. Furthermore we explicitly obtain the $O(m^2)$ finite mass corrections which are absent in ref. [7] and are crucial to obtain the right result in the very forward direction, where the initial and final radiation cones overlap and interfere. Our numerical results are obtained upon high precision (REAL*16) study of the kinematical configurations and require a sophisticated treatment of the integration around the singular forward region.

For a general treatment of radiative Bhabha cross sections in realistic setup at DAΦNE ($E_{cm} = 1020$ MeV), the following items must be considered (the contribution of the resonant process $e^+e^- \to \Phi \to e^+e^-\gamma$ is safely neglected everywhere):

(i) the cross section in the region $0 \leq \vartheta_- \leq \vartheta_-^{max}$, $E_-^{min} \leq E_- \leq E_-^{max}$, with $\vartheta_-^{max} \geq$ few $(1/\gamma)$, $E_-^{min} \simeq 200$ MeV and $E_-^{max} \simeq 450$ MeV, both totally inclusive on the positron and the photon and with acceptance cuts on them (this includes: single tagging rates for small angle scattered electron (SAST), double tagging rates for both electron and positron at small angle (SADT), coincidence rate of electron and photon in the forward direction (SAEPC));

(ii) the cross section for the electron in the small angle region defined above and the positron at large angle (SLDT), in particular in the region covered by the detector KLOE [8] ($8.5° \leq \vartheta_+ \leq 171.5°$);

(iii) the cross section for both electron and positron at large angle ($8.5° \leq \vartheta_-, \vartheta_+ \leq 171.5°$), but accompanied by a photon of energy $E_\gamma \geq E_\gamma^{min}$ at a minimum angle δ

from any of the final state fermions (LLDT);

(iv) the cross section for the light spot (LS), i.e. photons detected in the forward direction with energy $E_\gamma \geq k_0$, with $k_0 \simeq O(20\ \mathrm{MeV})$;

(v) the proper matrix element for each item above in order to study Monte Carlo simulations of transport phenomena and so on.

On the other hand, what is available up to now in the literature can be summarized as follows:

(i) the double differential spectra $d^2\sigma/dE_-d\vartheta_-$ and $d^2\sigma/dE_\gamma d\vartheta_\gamma$ in the small angle region, analytically integrated over all phase space and hence completely inclusive over the positron-photon and electron-positron degrees of freedom respectively [5,6];

(ii) the radiative Bhabha squared matrix element, quoted as valid in all kinematical situations [7], but actually not suitable for the treatment of very small scattering angle situations;

(iii) improved soft photon approximation estimate of small angle radiative Bhabha scattering: a very simple and effective, albeit approximated, formula for the SAST [9].

From the above considerations, it emerges that the correct matrix element valid in the small angle region and a FORTRAN code able to compute various tagging cross sections, with the possibility of taking into account several sets of experimental cuts, are still missing and this defines our goal.

Our notation is as follows:

$$s = (p_+ + p_-)^2, \quad t = (p_+ - q_+)^2, \quad u = (p_+ - q_-)^2,$$
$$s' = (q_+ + q_-)^2, \quad t' = (p_- - q_-)^2, \quad u' = (p_- - q_+)^2,$$

where $p_{-(+)}$ and $q_{-(+)}$ are the four-momenta of the incoming and outgoing electron (positron).

The matrix element for radiative Bhabha scattering, including s and t diagrams, is known from a long time [7]. It can be written as:

$$|M_B^0|^2 = (4\pi\alpha)^3 \, [W_1 + W_2 + W_3] \, \frac{ss'(s^2 + s'^2) + tt'(t^2 + t'^2) + uu'(u^2 + u'^2)}{ss'tt'}, \qquad (1)$$

where the expression for W_1, W_2 and W_3 can be found in [7]. The matrix element of eq. (1) has been derived in the ultrarelativistic limit and hence is valid only when the angles between all the particles involved are large. When a radiated photon comes out collinear to any of the charged particles, on the contrary, it is necessary to keep also the terms of the form $m^2/(p_i \cdot k)^2$, since the dot-products become of order m^2 too. In ref. [7] a very simple and general recipe has been given, where the form of the relevant m^2 terms is connected to the form of the corresponding Born process. In particular the proper mass corrections to the "massless" radiative Bhabha scattering matrix element (1) can be cast

in the following form [7]:

$$C^m = -4(4\pi\alpha)^3 m^2 \left[\frac{1}{(p_- \cdot k)^2} \left(\frac{s'}{t} + \frac{t}{s'} + 1 \right)^2 + \frac{1}{(p_+ \cdot k)^2} \left(\frac{s'}{t'} + \frac{t'}{s'} + 1 \right)^2 \right.$$
$$\left. + \frac{1}{(q_- \cdot k)^2} \left(\frac{s}{t} + \frac{t}{s} + 1 \right)^2 + \frac{1}{(q_+ \cdot k)^2} \left(\frac{s}{t'} + \frac{t'}{s} + 1 \right)^2 \right]. \tag{2}$$

The matrix element (1) with the mass corrections (2) describes a wide range of kinematical situations but does not apply to very small electron scattering angles, which actually is one of the regions of experimental interest at DAΦNE. Indeed, let us consider the scattering process at very small angles, of order, say, m/E. In this case a photon collinear to the initial state electron is also collinear to the final state one, so that, for instance, $p_- \cdot k \simeq q_- \cdot k \simeq O(m^2)$ and hence the terms of the kind $m^2/(p_- \cdot k)/(q_- \cdot k)$ become of the same order of $m^2/(p_- \cdot k)^2$ or $m^2/(q_- \cdot k)^2$. From now on the terms of the kind $m^2/(p_- \cdot k)/(q_- \cdot k)$ will be referred to as the "off-diagonal mass terms". Their physical meaning is very clear: they are a contribution to the initial-final state interference, which become more and more important when the electron scattering angle goes to zero.

In order to clarify this point in more detail, let us consider the matrix element for radiative Bhabha scattering in the soft-photon-approximation (spa) and taking into account radiation by the electron line only. Then, as well known,

$$|M^{spa}(k)|^2 \approx |M_0|^2 \left[- j^\mu(k) j^\dagger_\mu(k) \right],$$

where $j^\mu(k)$ is the classical current

$$j^\mu(k) = \frac{ie}{(2\pi)^{3/2}} \left[\frac{p_-^\mu}{(p_- \cdot k)} - \frac{q_-^\mu}{(q_- \cdot k)} \right].$$

This leads to

$$|M^{spa}(k)|^2 = 4\pi\alpha |M_0|^2 \left[\frac{2m^2 - t}{(p_- \cdot k)(q_- \cdot k)} - m^2 \left(\frac{1}{(p_- \cdot k)^2} + \frac{1}{(q_- \cdot k)^2} \right) \right]. \tag{3}$$

On the other hand, the matrix element of eq. (1) with its mass corrections (2) in the same limit and discarding emission of photon from the positron line, leads to

$$|M_B^{spa}(k)|^2 = 4\pi\alpha |M_0|^2 \left[\frac{-t}{(p_- \cdot k)(q_- \cdot k)} - m^2 \left(\frac{1}{(p_- \cdot k)^2} + \frac{1}{(q_- \cdot k)^2} \right) \right]. \tag{4}$$

The comparison between eqs. (3) and (4) clearly shows that in eq. (4) the term $m^2/(p_- \cdot k)/(q_- \cdot k)$ is missing. Thus eq. (4) is a good approximation of eq. (3) only in the limit

$|t| \gg m^2$. Now, in the kinematical situations of small angle electron scattering described above (SAST, SADT or SAEPC) the minimum four-momentum exchange t_0 is given by

$$|t_0| = \frac{m^6 x^2}{s^2(1-x)^2}, \qquad x = E_\gamma/E. \tag{5}$$

Therefore it is clear that the matrix element of eq. (4), or better the complete hard-photon result of eq. (1) with the mass corrections of eq. (2), is not adequate for describing the physics of Bhabha scattering at very small angles.

Let us consider now the general problem of small angle radiative Bhabha. The Born cross section for the elastic process $e^+e^- \to e^+e^-$ can be written as

$$\frac{d\sigma_0}{dt} = \frac{4\pi\alpha^2}{s^2}\left[\frac{s^2+u^2}{2t^2} + \frac{u^2+t^2}{2s^2} + \frac{u^2}{st}\right], \tag{6}$$

which is derived from t and s channel diagrams. The t^{-2} terms obviously dominate while the s channel diagrams and the $s-t$ interference contributions are suppressed in the forward direction by a factor (m^2/s) at least. Moreover, in the case of SAST, SADT and SAEPC, for kinematical reasons the only mass-divergent graphs are those where the initial or final state electron radiates and this is a gauge-invariant subset of all the diagrams.

Based on these arguments, the correct squared matrix element has been computed by using SCHOONSCHIP [10]. Our final result, up to $O(m^2)$ accuracy and including off-diagonal mass terms, can be written as

$$\begin{aligned}|M|^2 =& |M_B^0|^2 + C^m \\ &- \frac{(8\pi\alpha)^3 m^2}{2(p_- \cdot k)(q_- \cdot k)}\left[\frac{2su+3t'^2}{t^2} + \frac{s+u-2t'}{t} + 1\right],\end{aligned} \tag{7}$$

with $|M_B^0|^2$ and C^m given in eqs. (1) and (2). The matrix element of eq. (7) in the soft approximation naturally recovers the result of eq. (3) in the limit of single electron line radiation.

Let us discuss eq. (7) in detail. In the SLDT case, where for kinematical reasons no mass divergences appear, the ultrarelativistic matrix element of eq. (1) can be safely used. In the LLDT case mass divergences do appear but the condition $|t| \gg m^2$ is fulfilled so that the correct matrix element is given by (1) with the mass corrections (2). In all the other cases (SAST, SADT, SAEPC and LS) one has both mass divergences and very small angles, so that the full matrix element of eq. (7), which includes the off-diagonal mass corrections, must be used.

All the above results have been implemented in the FORTRAN code PHIPHI [11]. Let us compare our results with those already existing in the literature and discuss some implications of phenomenological interest.

In Fig. 1 the total cross section of small angle single tagging at DAΦNE obtained by integrating the electron energy over the range $\Delta E_- = E_-^{max} - E_-^{min} = 190$ MeV is shown as a function of the maximum electron energy E_-^{max}. The solid and dashed lines correspond

to the integration of the spectrum $d^2\sigma/dE_-d\vartheta_-$ of ref. [6] in two different domains of the electron scattering angle, namely $0 < \vartheta_- < 1$ mrad (dashed line) and $0 < \vartheta_- < 20$ mrad (solid line). Our results, obtained by means of the program PHIPHI, are represented by the open circles and squares showing a fully satisfactory agreement. For the energy and angle intervals of interest at DAΦNE, i.e. $210 < E_- < 400$ MeV and $250 < E_- < 440$ MeV with $\vartheta_-^{max} = 20$ mrad the total cross section is about 35, 50 mb respectively.

Fig. 2 shows a comparison for the total cross section of SAST between the results of ref. [9] and ours, or equivalently those of ref. [6], obtained with $0 < \vartheta_- < 1$ mrad , $0 < \vartheta_- < 2$ mrad and $0 < \vartheta_- < 20$ mrad and the electron energy within $\Delta E_- = E_-^{max} - E_-^{min} = 190$ MeV, as a function of the maximum electron energy E_-^{max}. The approximate formula of ref. [9] provides a good estimate of the SAST cross section with an accuracy of order 5 - 10 % when the kinematical configuration proposed in ref. [4] ($0 \leq \vartheta_- \leq 20$ mrad, 250 MeV $\leq E_- \leq 440$ MeV) is assumed. In the limit of small electron scattering angles ($\vartheta \leq 2$ mrad) the relative deviation decreases as E_-^{max} increases, consistently with the soft, collinear and no-recoil approximation adopted in ref. [9].

The total cross section for photons emitted in the forward region is shown in Fig. 3. The results are obtained by integrating the photon energy E_γ over the range $\Delta E_\gamma = E_b - E_\gamma^{min}$ as a function of the minimum photon energy E_γ^{min}. The different curves correspond to ϑ_γ in the regions $0 < \vartheta_\gamma < 1$ mrad (dashed line), $0 < \vartheta_\gamma < 2$ mrad (dotted line), $0 < \vartheta_\gamma < 3$ mrad (dash - dotted line), $0 < \vartheta_\gamma < 8.5^o$ (solid line).

In Tab. 1 we report the total cross section of small angle electron-photon double tagging obtained by integrating the photon polar angle ϑ_γ over the range $0 < \vartheta_\gamma < \vartheta_\gamma^{max}$ for different values of ϑ_γ^{max}. The electron scattering angle and energy are integrated over the regions $0 < \vartheta_- < 20$ mrad and $250 < E_- < 440$ MeV. In the second column σ/σ_{tot} is the fraction of the SAEPC cross section with respect to the total cross section of SAST.

In Tab. 2 the SLDT total cross section is reported. The results are obtained by integrating ϑ_- and ϑ_+ over the regions $0 < \vartheta_- < 20$ mrad and $8.5^o < \vartheta_+ < 171.5^o$, and the electron energy within $\Delta E_- = E_-^{max} - E_-^{min} = 190$ MeV, for different value of E_-^{max}.

In Tab. 3 the total cross section of LLDT is shown for $8.5^o < \vartheta_\pm < 171.5^o$, and $\Delta E_\gamma = E_b - E_\gamma^{min}$ for different values of E_γ^{min}. The constraint $\vartheta_{\gamma e^-}, \vartheta_{\gamma,e^+} > \delta$ is imposed, where δ is the half opening angle giving the angular resolution of the calorimeter (events with photons collinear to one of the final state fermions within an angle δ are rejected).

As a conclusion, we have presented an analysis of radiative Bhabha scattering at DAΦNE energies, with particular emphasis on the very forward region. We have explicitly computed the off-diagonal mass corrections required in that kinematical region and performed a phenomenological study of several configurations of relevant interest for $\gamma\gamma$ physics experiments at DAΦNE. A more detailed analysis will be given elsewhere.

Many stimulating discussions with D. Babusci and A. Zallo are gratefully acknowledged. We would like to thank INFN, Sezione di Pavia, for having provided computer resources and, in particular, V. Filippini and A. Fontana for having allowed the use of IBM RISC/350.

References

[1] See, for example, The DAΦNE Physics Handbook, L. Maiani, G. Pancheri and N. Paver Eds., and references therein.

[2] G. Vignola in Proceedings of the Workshop on Physics and Detectors for DAΦNE, Frascati, April 9 - 12, 1991, G Pancheri Ed.

[3] F. Anulli et al., ref. [1], Vol. II, pg. 435.

[4] G. Alexander et al., *Two Photon Physics Capabilities of KLOE at DAΦNE*, LNF-93/030(P).

[5] G. Altarelli and F. Buccella, Nuovo Cimento 34 (1964) 1337.

[6] V. N. Baier, V. S. Fadin, V. A. Khoze and E. A. Kuraev, Physics Report 78 (1981) 293.

[7] F. A. Berends, R. Kleiss, P. De Causmaecker, R. Gastmans, W. Trooost and T. T. Wu, Nucl. Phys. B 206 (1982) 61 and references therein. See also R. Gastmans and T. T. Wu, "The Ubiquitous Photon: Helicity Method for QED and QCD", Oxford Science Pub., 1990.

[8] KLOE, A General Purpose Detector for DAΦNE, LNF 92/019(R).

[9] G. Pancheri, *Estimate of Small Angle Radiative Bhabha Scattering at DAΦNE*, LNF - 93/024(P), June 1993.

[10] *SCHOONSCHIP, A Program For Symbol Handling* by M. Veltman, see H. Strubbe, Comp. Phys. Comm. 8 (1974) 1.

[11] G. Montagna, O. Nicrosini and F. Piccinini, *PHIPHI - A Program For Computing Radiative Bhabha Scattering Cross Sections at DAΦNE*, in preparation.

Figure and table captions

Fig. 1 Total cross section of small angle single tagging at DAΦNE (E_{cm} = 1020 MeV), obtained by integrating the electron scattering angle in the range $0 < \vartheta_- < 1$ mrad (dashed line) and $0 < \vartheta_- < 20$ mrad (solid line), and the electron energy over the range $\Delta E_- = E_-^{max} - E_-^{min} = 190$ MeV as a function of the maximum electron energy E_-^{max}. The open circles and squares are the results of the present analysis with the numerical error contained within the markers; the solid and dashed lines correspond to the integration of the spectrum of ref. [6].

Fig. 2 Comparison for the total cross section of small angle single tagging between the results of ref. [9] and ours, or equivalently those of ref. [6], obtained by integrating the electron scattering angle in the range $0 < \vartheta_- < 1$ mrad , $0 < \vartheta_- < 2$ mrad and $0 < \vartheta_- < 20$ mrad and the electron energy within $\Delta E_- = E_-^{max} - E_-^{min} = 190$ MeV, as a function of the maximum electron energy E_-^{max}. The relative deviation is defined as: $2\,(\sigma^{[9]} - \sigma)/(\sigma^{[9]} + \sigma)$

Fig. 3 Total cross section for the photon in the forward region obtained by integrating ϑ_γ in the regions $0 < \vartheta_\gamma < 1$ mrad (dashed line), $0 < \vartheta_\gamma < 2$ mrad (dotted line), $0 < \vartheta_\gamma < 10$ mrad (dash - dotted line), $0 < \vartheta_\gamma < 8.5^o$ (solid line) and E_γ over the range $\Delta E_\gamma = E_b - E_\gamma^{min}$ as a function of the minimum photon energy E_γ^{min}.

Tab. 1 Total cross section of small angle electron-photon double tagging obtained by integrating the photon polar angle ϑ_γ over the range $0 < \vartheta_\gamma < \vartheta_\gamma^{max}$ for different values of ϑ_γ^{max}. The electron energy and scattering angle are integrated over the regions $0 < \vartheta_- < 20$ mrad and $250 < E_- < 440$ MeV. In the second column σ/σ_{tot} is the percent contribution of the electron-photon double tagging cross section with respect the total cross section of small angle single tagging.

Tab. 2 Total cross section of small-large angle electron-positron double tagging obtained by integrating ϑ_- and ϑ_+ over the regions $0 < \vartheta_- < 20$ mrad and $8.5^o < \vartheta_+ < 171.5^o$ respectively, and the electron energy within $\Delta E_- = E_-^{max} - E_-^{min} = 190$ MeV, for different value of E_-^{max}.

Tab. 3 Total cross section of large-large angle electron-positron double tagging obtained by integrating $\vartheta_\pm$ in the range $8.5^o < \vartheta_\pm < 171.5^o$, the photon energy within $\Delta E_\gamma = E_b - E_\gamma^{min}$ for different value of E_γ^{min} and by imposing the constraint $\vartheta_{\gamma e^-}, \vartheta_{\gamma e^+} > \delta$, where δ is the half-opening angle giving the angular resolution of the calorimeter (events with photons collinear to one of the final state fermions within an angle δ are rejected).

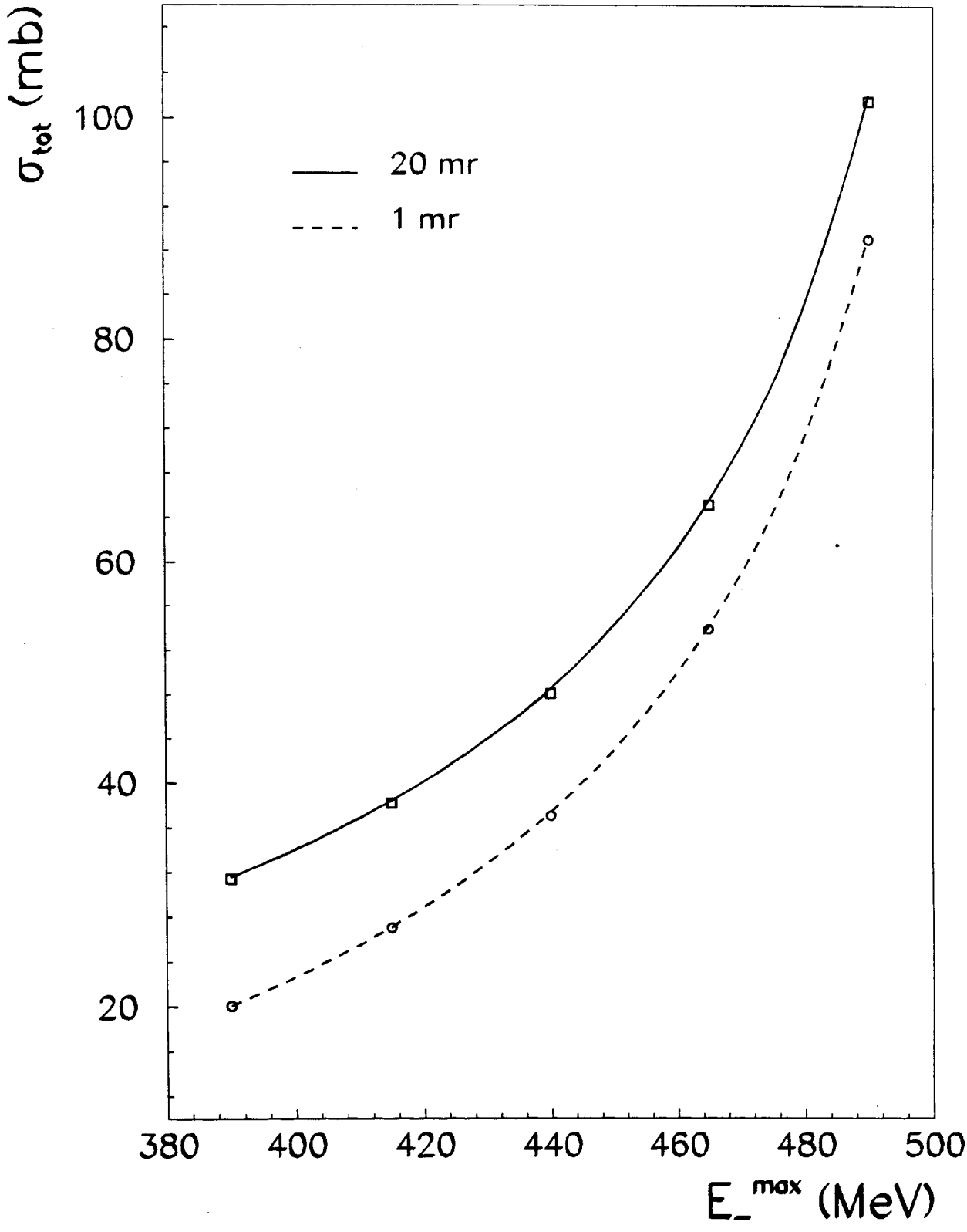
σtot (mb)
100
80
60
40
20
20 mr
1 mr
380
400
420
440
460
480
500
E_max (MeV)

FIG. 1

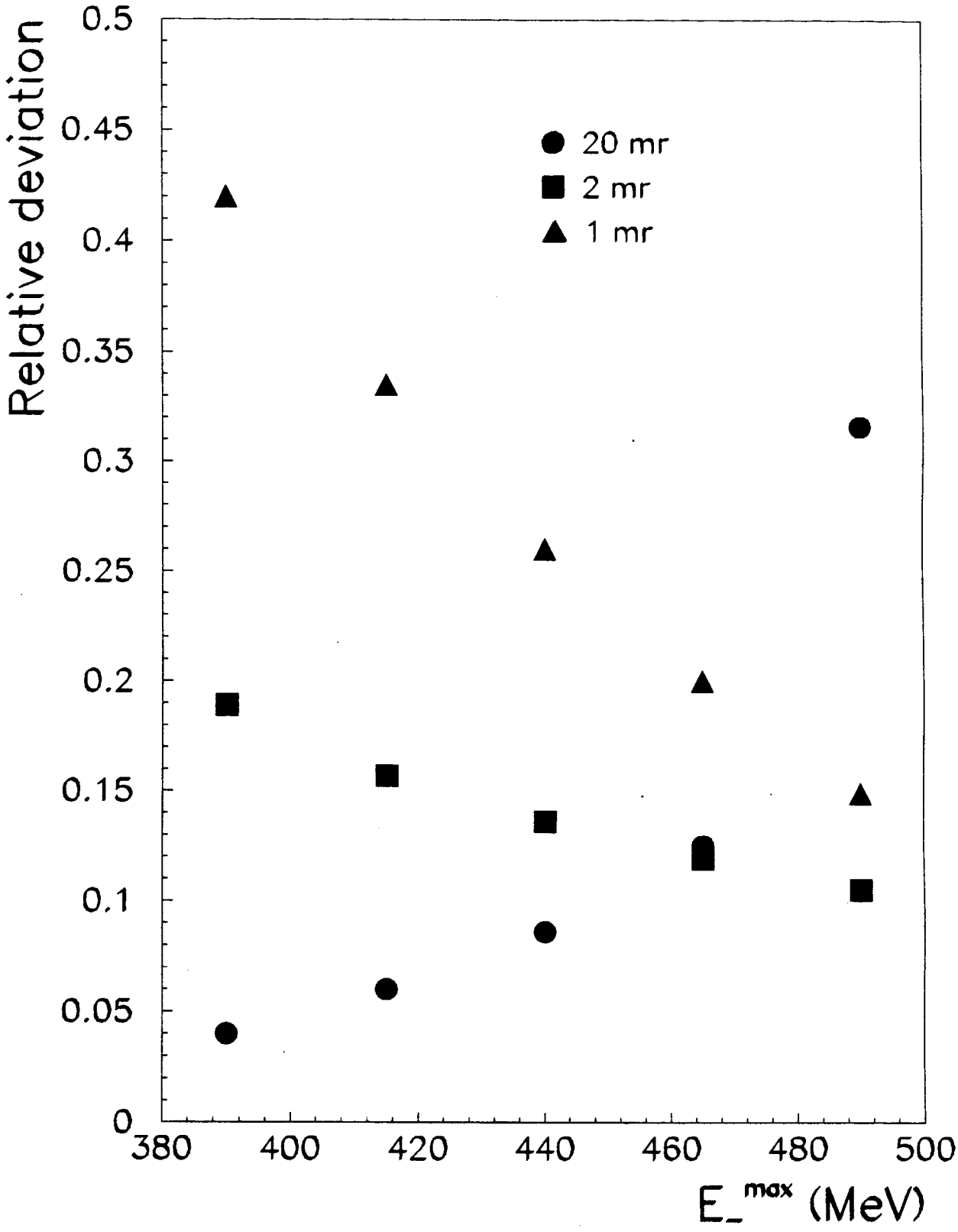
Relative deviation
0.5
0.45
0.4
0.35
0.3
0.25
0.2
0.15
0.1
0.05
0
380
400
420
440
460
480
500
E_max (MeV)
20 mr
2 mr
1 mr

FIG. 2

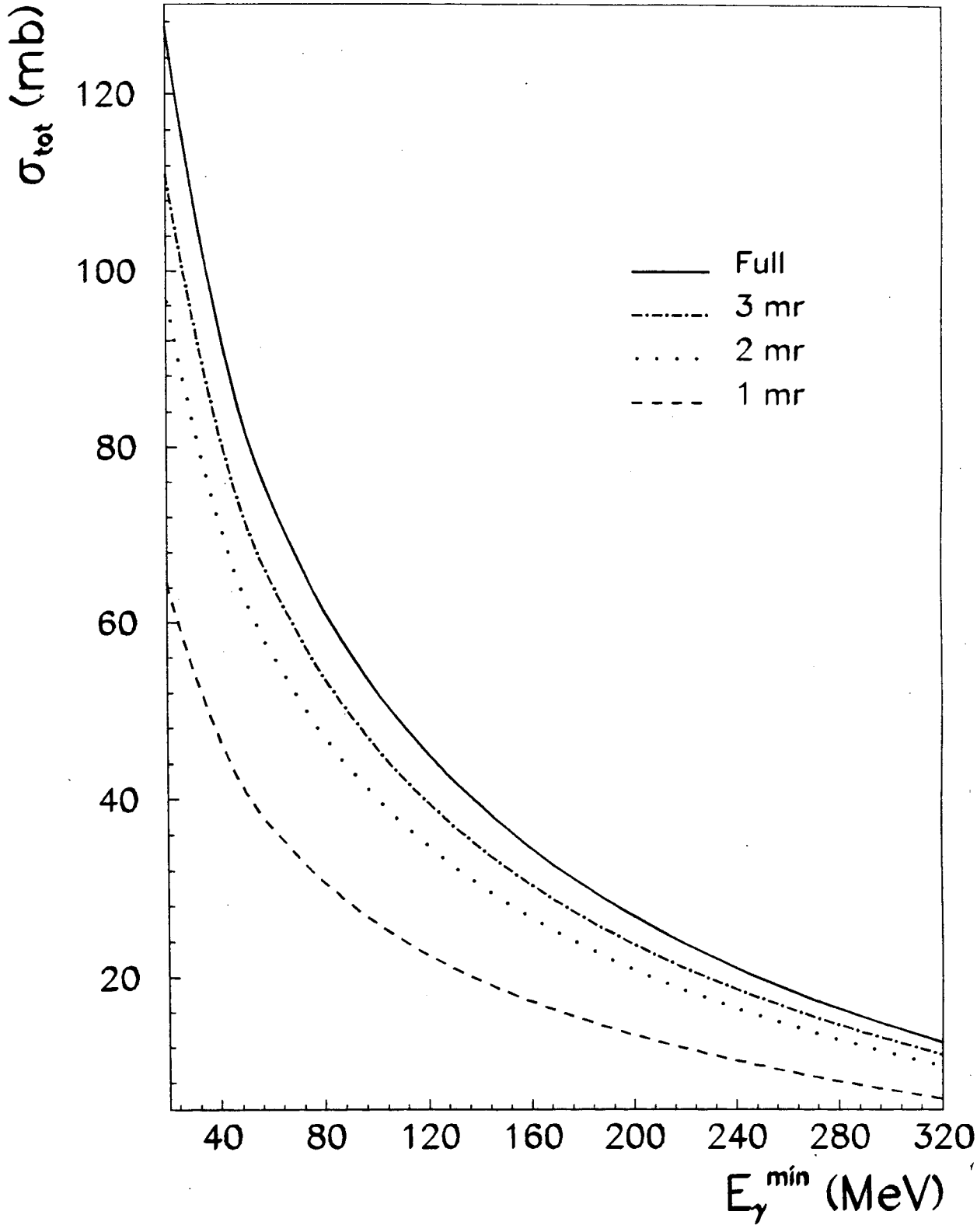
σ_{tot} (mb)
120
100
80
60
40
20
Full
3 mr
2 mr
1 mr
40
80
120
160
200
240
280
320
E_γ^{min} (MeV)

FIG. 3

Electron-photon small angle tagging		
$0 < \vartheta_- < 20$ mrad, $250 < E_- < 440$ MeV		
ϑ_γ^{max}	σ (mb)	σ/σ_{tot}
1 mrad	24.23 ± 0.24	49.96 %
2 mrad	39.22 ± 0.28	80.87 %
3 mrad	42.13 ± 0.42	86.87 %
10 mrad	47.81 ± 0.42	98.58 %
8.5°	48.32 ± 0.29	99.63 %

Tab. 1

Electron-positron small-large angle tagging	
$0 < \vartheta_- < 20$ mrad, $8.5^o < \vartheta_+ < 171.5^o$	
E_-^{max} (MeV)	σ (nb)
390	25 ± 0.3
415	41 ± 0.4
440	72 ± 0.7
465	155 ± 1.6
490	548 ± 5.8

Tab. 2

Electron-positron large-large angle tagging	
$8.5^o < \vartheta_\pm < 171.5^o$, $\delta = 0.5^o$	
E_γ^{min} (MeV)	σ (μb)
2	15.5 ± 0.6
5	12.6 ± 0.5
10	10.4 ± 0.4
50	5.5 ± 0.2
100	3.5 ± 0.1

Tab. 3